Evolution of a Pathway to Novel Long-Chain Carotenoids

Daisuke Umeno* and Frances H. Arnold

Division of Chemistry and Chemical Engineering, California Institute of Technology, Pasadena, California 91125

Using methods of laboratory evolution to force the C_{30} carotenoid synthase CrtM to function as a C_{40} synthase, followed by further mutagenesis at functionally important amino acid residues, we have discovered that synthase specificity is controlled at the second (rearrangement) step of the two-step reaction. We used this information to engineer CrtM variants that can synthesize previously unknown C_{45} and C_{50} carotenoid backbones (mono- and diisopentenylphytoenes) from the appropriate isoprenyldiphosphate precursors. With this ability to produce new backbones in *Escherichia coli* comes the potential to generate whole series of novel carotenoids by using carotenoid-modifying enzymes, including desaturases, cyclases, hydroxylases, and dioxygenases, from naturally occurring pathways.

Carotenoids are natural pigments with important biological activities (4, 10, 16, 17). Most are based on a 40-carbon (C_{40}) phytoene backbone produced by condensation of 2 molecules of geranylgeranyldiphosphate (GGDP; $C_{20}PP$), a reaction catalyzed by the carotenoid synthase CrtB (Fig. 1). The vast majority of the >700 known carotenoids (9) arise as a result of different types and levels of modification of the C_{40} backbone, catalyzed by promiscuous (downstream) carotenoid biosynthetic enzymes (5). A few bacteria, notably *Staphylococcus* and *Heliobacterium* spp. (23, 24), have a C_{30} pathway, which starts with the CrtM synthase-catalyzed condensation of 2 molecules of farnesyldiphosphate (FDP; $C_{15}PP$) to form 4,4′-diapophytoene. Yet other bacteria (such as *Corynebacterium* and *Halobacterium* spp.) are known to accumulate C_{50} carotenoids, but these longer-chain structures are biosynthesized starting from the C_{40} structure by the addition of 2 C_5 (isoprene) units (14). Various longer isoprenyldiphosphates are made by different organisms (30) and are potential precursors for longer-chain carotenoids. They are precursors to other biosynthetic pathways, however, and no known carotenoids are derived from them. Thus, carotenoid size is tightly controlled by the carotene synthase reaction (20, 27).

To create new pathways for the biosynthesis of carotenoids with backbones larger than C_{40}, we focused on engineering the carotenoid synthase to accept longer diphosphate substrates. Very little is known of the structure or basis for the specificity of these membrane-associated enzymes. Using random mutagenesis and a functional complementation screen for C_{40} synthase activity, however, we identified single-amino-acid substitutions in the C_{30} synthase CrtM (F26L or F26S) that confer the C_{40} function (27). By repeating this experiment with a random mutant library that was free from mutation at F26, we recently found two more amino acid substitutions, W38C and E180G, that confer the same phenotype (26). Upon further mutagenesis at these three residues, we show here that the specificity of the carotenoid synthase CrtM is controlled at the

second (rearrangement) step of its two-step reaction. Furthermore, we have engineered synthase variants that can make previously unknown C_{45} and C_{50} carotenoid backbones (mono- and diisopentenylphytoenes) from the appropriate C_{20} and C_{25} isoprenyldiphosphate precursors. With this ability to produce the new backbones in *Escherichia coli* comes the potential to generate whole series of novel carotenoids upon addition of carotenoid-modifying enzymes to the engineered pathway.

MATERIALS AND METHODS

Materials. The *crtE* (GGDP synthase), *crtB* (phytoene synthase), and *crtI* (phytoene desaturase) genes are from *Erwinia uredovora*, as described elsewhere (21, 27). *crtM* (diapophytoene synthase) and *crtN* (diapophytoene desaturase) are from *Staphylococcus aureus* (25, 27). *Bacillus stearothermophilus* farnesyldiphosphate synthase (BsFDS) was PCR cloned from genomic DNA (ATCC 12980) according to the literature (13). AmpliTaq polymerase (Perkin-Elmer, Boston, Mass.) was used for mutagenic PCR, while Vent polymerase (New England Biolabs, Beverly, Mass.) was used for cloning PCR.

Plasmid construction. *crtN* was subcloned into the *EcoRI/NcoI* site of pUC-modII (21), resulting in pUC-*crtN*. *crtB* was removed from previously constructed pUC-*crtE-crtB-crtI* (27) to give pUC-*crtE-crtI*. From these two plasmids, genes and promoters (*lacP-crtN* and *lacP-crtE-crtI*, respectively) were PCR amplified and subcloned into the *SalI* site of pACYC184, resulting in pAC-*crtN* and pAC-*crtI-crtE*, respectively. Carotene synthase genes (*crtB* and *crtM*) were cloned into the *XbaI/XhoI* site in pUC18Nmod (27), resulting in pUC-*crtB* and pUC-*crtM*. Plasmid pUC-*BsFDS*$_{Y81A}$ was constructed by subcloning the Y81A mutant of BsFDS (followed by a ribosome binding site) into the *EcoRI/NcoI* site of pUCmod. *crtB* or *crtM* was subcloned into the *XbaI/XhoI* site of this construct, resulting in pUC-*crtB-BsFDS*$_{Y81A}$ and pUC-*crtM-BsFDS*$_{Y81A}$.

Site-directed mutants. PCR-based site saturation or substitution mutagenesis was performed on F26 (TTT), W38 (TGG), and E180 (GAA) by using the ExSite method (Stratagene). Some site-directed mutants were obtained from the saturation mutagenesis library, but the majority were synthesized using individual primers with the appropriate codon at the targeted site. Double and triple mutants were constructed by repeated site-directed mutagenesis. Selected mutants were subcloned into the *XbaI/XhoI* site of pUC-*BsFDS*$_{Y81A}$ to produce pUC-[*crtM*]-*BsFDS*$_{Y81A}$ (square brackets indicate a *crtM* mutant).

Evaluating the C_{30} and C_{40} activities of CrtM variants. To measure C_{40} synthase activity, genes encoding CrtM and its variants were placed in the *XbaI-XhoI* site of pUC18Nm (27) and transformed into XL1 cells harboring pAC-*crtE-crtI*. Similarly, C_{30} synthase activity was evaluated upon transformation of pUC-*crtM* (or pUC-[*crtM*]) into XL1 cells harboring pAC-*crtN*. Colonies were lifted onto white nitrocellulose membranes (Pall, Port Washington, N.Y.) and grown at room temperature for an additional 12 to 24 h. Colonies were picked and cultured overnight in 96-well deep-well plates, each well containing 0.5 ml of liquid Luria-Bertani (LB) medium supplemented with carbenicillin and chloramphenicol (50 µg/ml each), and were shaken for 12 h at 37°C. A portion (20 µl)

* Corresponding author. Mailing address: Division of Chemistry and Chemical Engineering, California Institute of Technology, 210-41 1200 E. California Blvd, Pasadena, CA 91125. Phone: (626) 395-4162. Fax: (626) 568-8743. E-mail: umeno@cheme.caltech.edu.
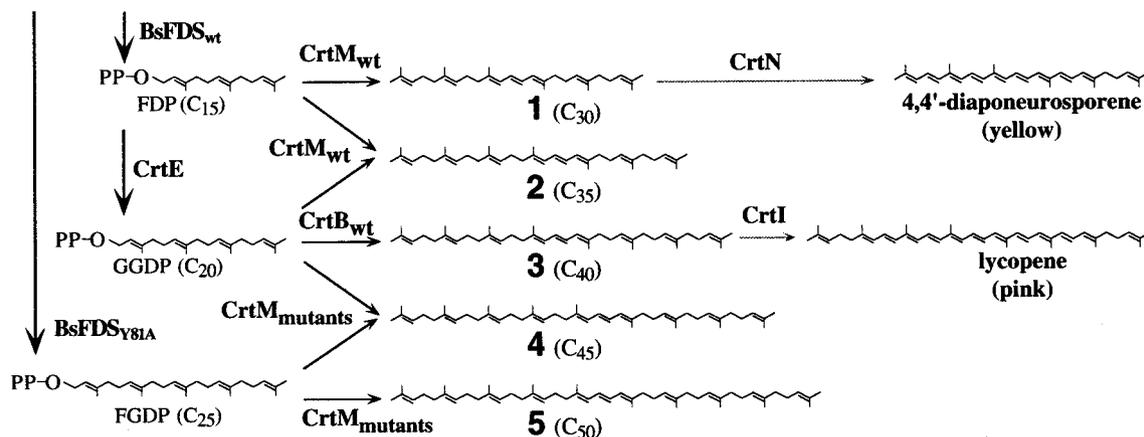
FIG. 1. Natural and unnatural pathways for carotenoid biosynthesis. In addition to natural C_{30} and C_{40} carotenoid pathways, C_{35}, C_{45}, and C_{50} carotenoid pathways have been constructed in *E. coli*. The number assigned to each carotenoid corresponds to those in Fig. 5. CrtN, dehydro-squalene (C_{30}) desaturase; CrtI, phytoene (C_{40}) desaturase.

from each preculture was inoculated into 2 ml of fresh Terrific Broth (TB) culture. After being shaken for 36 h at 30°C, cells were harvested and extracted with acetone (1 ml). The highest peak (475 nm) in each UV/visible spectrum was used to score C_{40} activity, while 470 nm was used for C_{30} activity. Values reported are averages from six independent experiments.

Carotenoid production and HPLC analysis. Plasmids (pUCs) were transformed into HB101 cells and grown on agar plates (LB) with carbenicillin (50 μg/ml) for 14 to 16 h. Fresh colonies were picked, inoculated into TB medium, and shaken for 12 h at 37°C. An aliquot (0.5 ml) of this preculture was inoculated into 150 ml of TB medium (in a 750-ml tissue culture flask; Falcon) and shaken at 30°C for 36 to 40 h. Wet cells were harvested from the culture, extracted with 20 ml of acetone, transferred to 10 ml of hexane, dried with anhydrous MgSO$_4$, and concentrated in a rotary evaporator. An aliquot of extract was passed through a Spherisorb ODS2 column (250 by 4.6 mm; particle diameter, 5 μm; Waters, Milford, Mass.) and eluted with an acetonitrile-isopropanol mixture (60:40 [vol/vol]) at a flow rate of 1 ml/min by using an Alliance–HPLC (high-performance liquid chromatography) system (Waters) equipped with a photodiode array detector. For analysis of molecular mass, a Series 1100 LC/MSD (Hewlett-Packard/Agilent, Palo Alto, Calif.) coupled with an atmospheric pressure chemical ionization (APCI) interface was used. The amount of each carotenoid was determined by comparing the HPLC chromatogram peak area (at 286 nm) to that of a β-carotene standard (at 450 nm). To obtain the molar quantity, the value thus obtained (β-carotene equivalent) was multiplied by $\varepsilon_{\beta\text{-carotene}}$ (138,900 cm^{-1} M^{-1} at 450 nm) divided by $\varepsilon_{\text{phytoene}}$ (49,800 cm^{-1} M^{-1} at 286 nm). Molar quantity was then converted to a weight value by multiplying by its molecular weight. The weights were then normalized to the dry cell mass of each culture.

RESULTS

C_{40} and C_{30} carotenoid synthase activities of CrtM variants. To probe how modifications at residues 26, 38, and 180 of *S. aureus* CrtM allow this C_{30} carotenoid synthase to condense two C_{20} precursors and function as a C_{40} synthase, we performed saturation mutagenesis at all three sites. Significant fractions of the F26X (where X stands for any amino acid) and W38X libraries (ca. 65 and 50%, respectively) showed a pink hue (due to accumulated lycopene) upon transformation into XL1 cells harboring pAC-*crtE-crtI*. In contrast, only 2 to 3% of the E180X library colonies showed a (weak) pink color, indicating that only a few amino acids (probably glycine alone) can positively contribute to the C_{40} synthase activity.

Eleven, 11, and 3 site-directed mutants were created at positions F26, W38, and E180, respectively (Fig. 2). These were
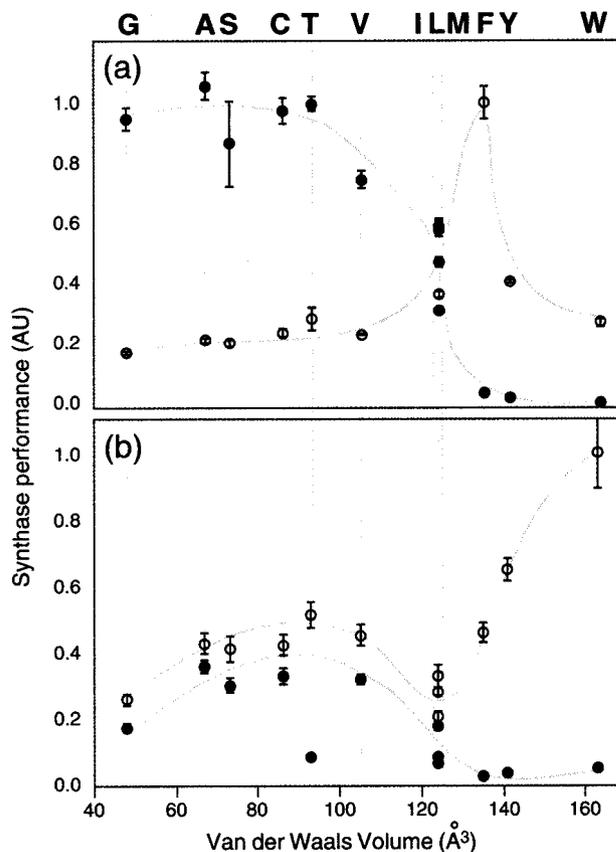

FIG. 2. Relationship between C_{40} or C_{30} synthase function and van der Waals volume of amino acid side chain at position 26 (a) and position 38 (b) in CrtM. Values for C_{40} function (solid circles) were obtained from the peak absorption (475 nm) of an acetone extract from XL1 cells harboring pAC-*crtE-crtI*. Similarly, C_{30} function (open circles) was obtained from the peak absorption of the acetone extract (470 nm) from XL1 cells harboring pAC-*crtN*. See Materials and Methods for more detail. Each data point is the average of six independent experiments. Error bars, standard deviations.

tested individually for their abilities to lead to pigment production in a C_{30} and a C_{40} pathway assembled in *E. coli.* To test C_{40} synthase performance, mutants were transformed into *E. coli* cells expressing the *E. uredovora* GGDP synthase CrtE and the C_{40} desaturase CrtI. Cells containing CrtM variants that have acquired C_{40} synthase activity accumulate lycopene. The pigmentation level was determined from the peak height (at 475 nm) of the acetone extract. Similarly, C_{30} synthase performance was evaluated from the pigmentation level of cells transformed with the genes for CrtM and the *S. aureus* C_{30} desaturase CrtN. Functional CrtM variants led to production of 4,4′-diapophytoene, which was quantified (470 nm) in the acetone extract. As shown in Fig. 2, replacement of F26 or W38 by a smaller amino acid significantly increased the C_{40} synthase activity of CrtM. C_{30} performance was the highest for wild-type CrtM and decreased with decreasing sizes of the amino acid residues at these positions. Thus, gain of C_{40} function by mutation of CrtM came at a cost to its C_{30} synthase activity.

CrtM generates 4,4′-diapophytoene (product 1) in two distinct steps: (i) abstraction of a diphosphate group from a prenyl donor, followed by head-to-head condensation of the donor and acceptor molecules, and (ii) rearrangement of the cyclic intermediate, followed by removal of a second diphosphate and a final carbocation quenching process (Fig. 3a). This mechanism is virtually identical to that of squalene synthase (SqS), the enzyme that catalyzes the first step in cholesterol biosynthesis. Indeed, when deprived of NADPH, SqS produces product 1 as the main product (3, 11). Carotene synthases are similar to SqS in sequence and predicted secondary structure; they probably share a common ancestor and have virtually identical folds. Although detailed biochemical information on SqS is available (3, 11), the basis of its specificity is also poorly understood. Mapped onto the crystal structure of human SqS (hSqS) (19), F26 and W38 appear in helices B and C. Both side chains point into the pocket that accommodates the second half-reaction (Fig. 3b). We reasoned that wild-type CrtM is able to perform the first half-reaction of phytoene (C_{40}) synthesis (condensation of 2 GGDP molecules to form prephytoenediphosphate) but that the reaction is prevented from going to completion by bulky residues which sterically inhibit the second, rearrangement step. When F26 or W38 is replaced with smaller or more flexible amino acids, the reaction can proceed, and phytoene is produced.

In both the C_{30} and C_{40} pathways, $M_{F26A/W38G}$ (CrtM with the F26A and W38G mutations) and $M_{F26A/W38A}$ performed more poorly than M_{F26A}, and $M_{F26G/W38G}$ and $M_{F26G/W38A}$ performed more poorly than M_{F26G} (Fig. 4). Thus, the combination of mutations at F26 and W38 appears to be harmful for the general performance of CrtM, probably due to perturbation of the reaction pocket, which decreases the overall catalytic activity.

Based on the SqS structure, E180 in CrtM is positioned outside the reaction pocket, closer to the location where the first half-reaction occurs (Fig. 3b). At this position, glycine is the only amino acid that allows CrtM to exhibit measurable C_{40} synthase activity. In contrast to the F26X and W38X mutants, which showed a marked decrease in C_{30} performance, M_{E180G} showed a slight increase in C_{30} synthase activity (data not shown). Thus, the E180G mutation positively affects CrtM
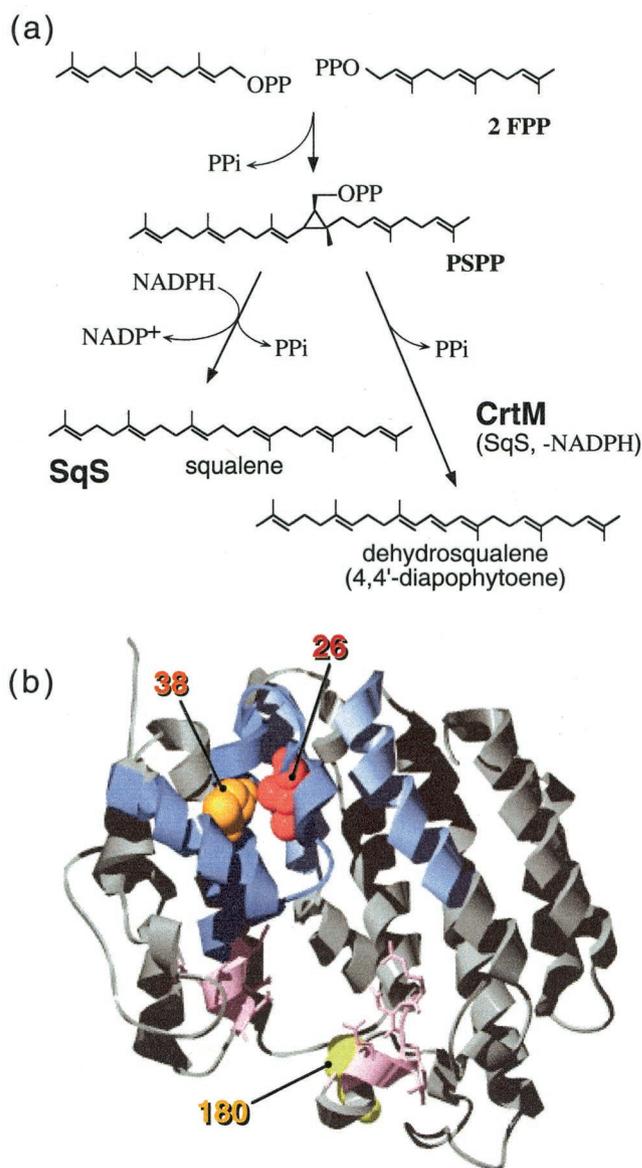

FIG. 3. (a) Reaction mechanism of SqS and CrtM. (b) Positions corresponding to F26, W38, and E180 of CrtM are shown in the crystal structure of hSqS (19). Residues depicted as pink are involved in the first half-reaction, while residues depicted as blue affect the second half-reaction.

performance in both the C_{30} and C_{40} contexts. In fact, for all tested CrtM variants (M_{F26G}, M_{F26A}, $M_{F26G/W38G}$, $M_{F26G/W38A}$, $M_{F26A/W38G}$, and $M_{F26A/W38A}$), addition of E180G enhanced pigmentation for the C_{30} and C_{40} pathways (Fig. 4).

CrtM variants generate longer (C_{45} and C_{50}) carotenoid backbones when supplied with the C_{25} precursor FGDP. Isoprenyldiphosphates are ubiquitous building units for thousands of natural products and cell components. Different isoprenyldiphosphate synthases catalyze the consecutive condensation of C_5 units to produce a wide range of isoprenyldiphosphates (C_{10} to $C_{\sim 20,000}$). Isoprenyldiphosphate synthases with different product size distributions are known, and the molecular
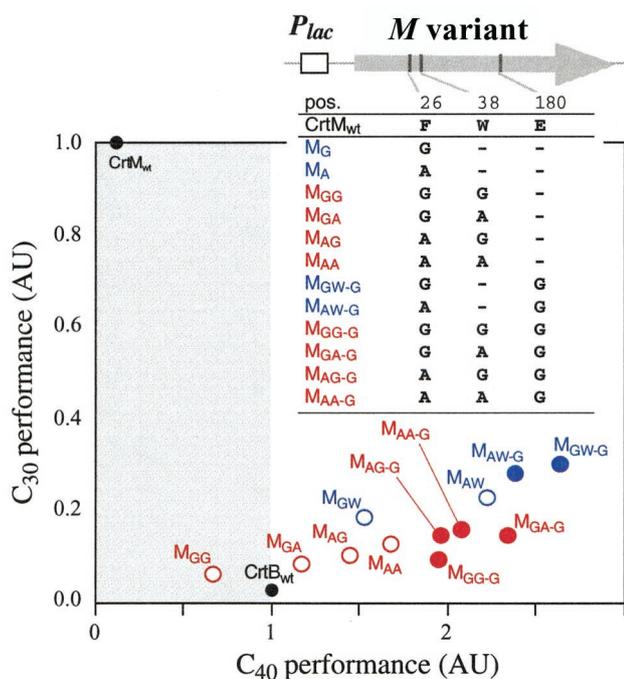
FIG. 4. Comparison of the performance (pigment production) of selected single, double, and triple mutants of CrtM in C_{30} and C_{40} pathways. For each of the CrtM variants, C_{40} synthase function (*x* axis) and C_{30} function (*y* axis) were measured as described in the text. Each value was normalized to the value of wild-type CrtB (CrtB$_{wt}$) and CrtM$_{wt}$, respectively. Variants with a mutation at F26 are shown in blue, while those with mutations at both F26 and W38 are in red. Open and solid circles, variants without and with the E180G mutation, respectively. Each data point represents the average of four independent experiments.
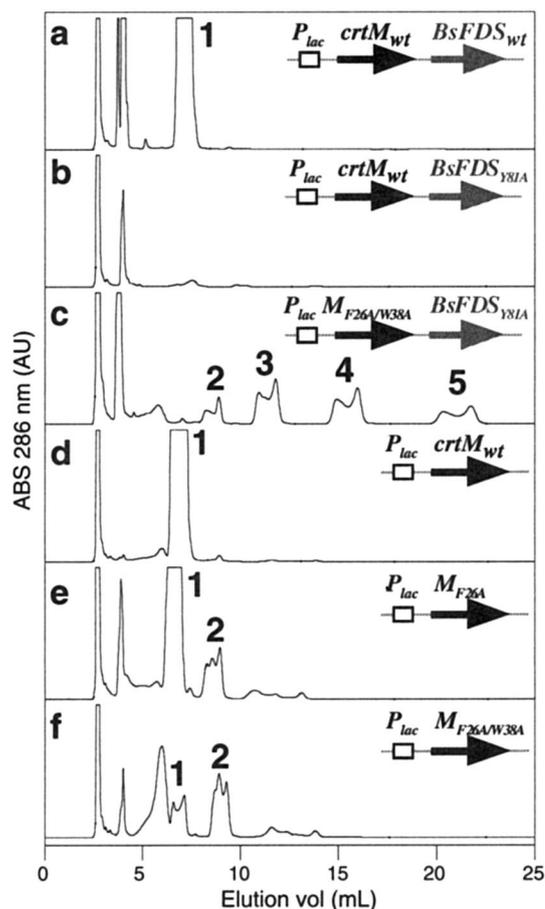

FIG. 5. HPLC analysis of carotenoids produced in *E coli* HB101 cells carrying plasmid pUC-*crtM$_{wt}$*-*BsFDS$_{wt}$* (a), pUC-*crtM$_{wt}$*-*BsFDS$_{Y81A}$* (b), pUC-*M$_{F26A/W38A}$*-*BsFDS$_{Y81A}$* (c), pUC-*crtM$_{wt}$* (d), pUC-*M$_{F26A}$* (e), or pUC-*M$_{F26A/W38A}$* (f). Individual compounds are as follows: peak 1, 4,4′-diapophytoene (M^+ at m/e = 409); peak 2, 4-apophytoene (M^+ at m/e = 476); peak 3, phytoene (M^+ at m/e = 544); peak 4, 16-isopentenylphytoene (M^+ at m/e = 612); peak 5, 16,16′-diisopentenylphytoene (M^+ at m/e = 680). Elution conditions were as follows: an ODS-2 column; flow rate, 1 ml/min; acetonitrile/2-propanol ratio, 60:40 (vol/vol). The detection wavelength was 286 nm.

basis of their product size determination is well understood (29). BsFDS is very specific and produces FDP almost exclusively, both in vitro and in vivo (13). Ohnuma et al. have shown, however, that the product specificity of BsFDS can be controlled by altering the size of the amino acid at position 81 (18). The Y81A BsFDS variant produces farnesylgeranyldiphosphate (FGDP; C_{25}DP) as the main product in vitro, with small amounts of GGDP. We observed that *E. coli* HB101 cells harboring pUC-*crtM$_{wt}$*-*BsFDS$_{Y81A}$* produced almost no carotenoids (Fig. 5b), while those harboring pUC-*crtM$_{wt}$*-*BsFDS$_{wt}$* produced product 1 at a high level, 1.1 mg/g (dry cell weight [DCW]) (Fig. 5a). The fact that no C_{30} carotenoids were observed indicates that FDP is not supplied for C_{30} carotenoid production, which we attribute to its redirection toward the longer isoprenyldiphosphates, catalyzed by BsFDS.

When coexpressed with BsFDS$_{Y81A}$, several CrtM variants with substitutions at positions 26 and 38 generated C_{35} (product 2) and C_{40} (product 3) carotenoids along with two novel carotenoids, products 4 and 5 (Fig. 5c). Based on their mass analysis (M^+ at m/e = 612 for product 4 and 680 for product 5), elution time, and characteristic absorption spectra (maximum peak at 286 nm), we conclude that products 4 and 5 are 16-isopentenylphytoene (the C_{45} carotenoid backbone, C_{20} plus C_{25}) and 16,16′-diisopentenylphytoene (C_{50} backbone, C_{25} plus C_{25}). The distribution of the different carotenoid backbones varied, depending on the synthase. Among the single mutants, M$_{F26A}$ produced the highest levels of product 4 (ca. 130 µg/g [DCW]) and product 5 (78 µg/g [DCW]) (Fig. 6). Combining mutations at positions 26 and 38 usually decreased the total carotenoid production. For example, HB101 cells harboring pUC-*M$_{F26A/W38A}$*-*BsFDS$_{Y81A}$* produced lower levels of carotenoids than cells with pUc-*M$_{F26A}$*-*BsFDS$_{Y81A}$*. However, the extent of decrease was negligible for products 4 and 5, while it was significant for products 2 and 3. Thus, in this system, more than half the carotenoids were longer-chain structures, products 4 (35%) and 5 (22%). This "shifted" size specificity was further confirmed by analyzing the products in the C_{30} pathway: when pUC-*M$_{F26A/W38A}$* was transformed into HB101 cells, a very small amount of product 1 was accumulated along with a smaller amount of product 2 (Fig. 5f). In contrast, cells harboring wild-type pUC-*crtM* and pUC-*M$_{F26A}$* accumulated a high level of product 1 (Fig. 5d and e).

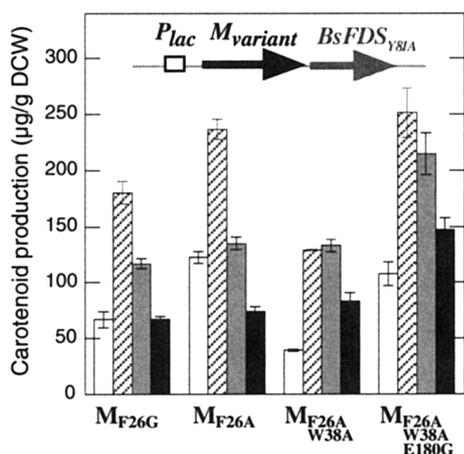Because the E180G substitution increases overall synthase

FIG. 6. Size distribution of carotenoid backbones synthesized by selected CrtM variants expressed with the Y81A mutant of BsFDS. Open bar, product 2 (C_{35}); striped bar, product 3 (C_{40}); shaded bar, product 4 (C_{45}); solid bar, product 5 (C_{50}). Values were obtained from HPLC peak areas of extracts from *E. coli* HB101 cells carrying pUC-[*crtM*]s-BsFDS$_{Y81A}$.

activity in the C_{30} and C_{40} pathways (Fig. 4), and because it is far from F26 or W38 (Fig. 3b), we anticipated that introduction of E180G to $M_{F26A/W38A}$ would enhance carotenoid production without altering the preference for larger (C_{45} or C_{50}) structures. Indeed, the highest production of products 4 (215 μg/g [DCW]) and 5 (147 μg/g [DCW]) was attained with HB101 cells harboring pUC- $M_{F26A/W38A/E180G}$-BsFDS$_{Y81A}$ (Fig. 6).

DISCUSSION

In previous work we showed that wild-type CrtM can produce a C_{35} carotenoid backbone in the presence of high levels of the C_{20} precursor GGDP (25). Various downstream enzymes (desaturases and cyclases) from the C_{30} and C_{40} carotenoid pathways were functional on this nonnatural substrate, which led to the production of a series of novel C_{35} carotenoids. Using directed evolution, with screening for altered pigment production, we were able to generate pathways for every possible C_{35} desaturation product. Thus, it appears that once a carotenoid backbone structure is created, downstream enzymes, either natural or engineered, can accept the new substrate, and whole series of novel carotenoids can be produced. With the action of carotenoid-modifying enzymes, including desaturases, cyclases, hydroxylases, and cleavage enzymes, on these new extended backbones, it should be possible to double or even triple the diversity of the carotenoid kingdom.

It is argued that, over evolutionary time scales, secondary metabolic pathways explore chemical diversity via gene duplication and mutation of biosynthetic enzymes and thereby discover compounds that confer fitness advantages (28). Secondary metabolic pathways in fact seem to have evolved features that facilitate efficient exploration of new chemical structures (8). For example, the biosynthetic enzymes often accept a range of substrates and/or produce a variety of products from a single substrate (11, 22); this "promiscuous" behavior allows

whole series of novel metabolites to emerge upon minimal change in an existing pathway (1, 2, 7, 12, 15, 25). In contrast, some enzymes, frequently those in key positions at the start of a pathway, show considerable stringency in the substrates they accept (6, 20, 27). This upstream specificity serves to limit the production of unwanted by-products. For carotenoids, the highly specific synthase reaction appears to be the major point of control over product diversity. Other isoprenoid pathways are similar to the carotenoid pathways in that the first pathway-specific enzymes are very specific in their substrate selection and thereby channel the entire pathway to a particular product (6). Engineering of these specificity-controlling enzymes is likely to be the most efficient way to expand these other isoprenoid biosynthetic pathways to create new metabolites.

We do not know why the new carotenoid pathways that we generated in the laboratory are not seen in nature. Combination of two engineered enzymes, with as little as one amino acid substitution each, led to the production of novel carotenoid backbones, unambiguously showing that whole new carotenoid pathways can emerge and can do so rapidly. It is likely that C_{45} and C_{50} carotenoid pathways have been invented by nature but that we have not yet discovered them. Perhaps they have been invented and then discarded, because the producing organisms did not benefit. The benefits to human inventors of these pathways, however, may be significant. In addition to the expected higher antioxidant activity (2) and possible hormonal effects (4, 10), larger chromophores for carotenoids (19 conjugated double bonds for C_{50} carotenoids, 23 for C_{60}) will extend the color range of these natural pigments. A variety of isoprenyldiphosphate synthases that produce isoprenyldiphosphates of different sizes (e.g., $C_{30}DP$, $C_{35}DP$, $C_{40}DP$, $C_{45}DP$, $C_{55}DP$, and natural rubber) are available (30); these compounds could, in principle, serve as substrates for engineered synthases.

Although impressive in number, the known products of secondary metabolic pathways account for only a tiny fraction of the structures that could be produced. Engineering the upstream biosynthetic enzymes to accept new substrates allows us to generate whole new pathways and access very large numbers of secondary metabolites that are not known in nature but should be chemically, and biologically, possible.

REFERENCES

1. **Albrecht, M., S. Takaichi, N. Misawa, G. Schnurr, P. Boger, and G. Sandmann.** 1997. Synthesis of atypical cyclic and acyclic hydroxy carotenoids in *Escherichia coli* transformants. J. Biotechnol. **58:**177–185.
2. **Albrecht, M., S. Takaichi, S. Steiger, Z. Y. Wang, and G. Sandmann.** 2000. Novel hydroxycarotenoids with improved antioxidative properties produced by gene combination in *Escherichia coli.* Nat. Biotechnol. **18:**843–846.
3. **Blagg, B. S. J., M. B. Jarstfer, D. H. Rogers, and C. D. Poulter.** 2002. Recombinant squalene synthase. A mechanism for the rearrangement of presqualene diphosphate to squalene. J. Am. Chem. Soc. **124:**8846–8853.
4. **Blount, J. D., N. B. Metcalfe, T. R. Birkhead, and P. F. Surai.** 2003. Carotenoid modulation of immune function and sexual attractiveness in zebra finches. Science **300:**125–127.
5. **Britton, G.** 1998. Overview of carotenoid biosynthesis, p. 13–147. *In* G. Britton, S. Liaaen-Jensen, and H. Pfander (ed.), Carotenoids, vol. 3. Biosynthesis. Birkhauser Verlag, Basel, Switzerland.
6. **Chappell, J.** 1995. Biochemistry and molecular-biology of the isoprenoid biosynthetic-pathway in plants. Annu. Rev. Plant Physiol. Plant Mol. Biol. **46:**521–547.

7. **Croteau, R., F. Karp, K. C. Wagschal, D. M. Satterwhite, D. C. Hyatt, and C. B. Skotland.** 1991. Biochemical characterization of a spearmint mutant that resembles peppermint in monoterpene content. Plant Physiol. **96:**744–752.

8. **Firn, R. D., and C. G. Jones.** 2000. The evolution of secondary metabolism—a unifying model. Mol. Microbiol. **37:**989–994.

9. **Hornero-Me'ndez, D., and G. Britton.** 2002. Involvement of NADPH in the cyclization reaction of carotenoid biosynthesis. FEBS Lett. **515:**133–136.

10. **Ishimi, Y., M. Ohmura, X. X. Wang, M. Yamaguchi, and S. Ikegami.** 1999. Inhibition by carotenoids and retinoic acid of osteoclast-like cell formation induced by bone-resorbing agents in vitro. J. Clin. Biochem. Nutr. **27:**113–122.

11. **Jarstfer, M. B., D. L. Zhang, and C. D. Poulter.** 2002. Recombinant squalene synthase. Synthesis of non-head-to-tail isoprenoids in the absence of NADPH. J. Am. Chem. Soc. **124:**8834–8845.

12. **Komori, M., R. Ghosh, S. Takaichi, Y. Hu, T. Mizoguchi, Y. Koyama, and M. Kuki.** 1998. A null lesion in the rhodopin 3,4-desaturase of *Rhodospirillum rubrum* unmasks a cryptic branch of the carotenoid biosynthetic pathway. Biochemistry **37:**8987–8994.

13. **Koyama, T., S. Obata, M. Osabe, A. Takeshita, K. Yokoyama, M. Uchida, T. Nishino, and K. Ogura.** 1993. Thermostable farnesyl diphosphate synthase of *Bacillus stearothermophilus*—molecular cloning, sequence determination, overproduction, and purification. J. Biochem. (Tokyo) **113:**355–363.

14. **Krubasik, P., M. Kobayashi, and G. Sandmann.** 2001. Expression and functional analysis of a gene cluster involved in the synthesis of decaprenoxanthin reveals the mechanisms for C_{50} carotenoid formation. Eur. J. Biochem. **268:**3702–3708.

15. **Lee, P. C., A. Z. R. Momen, B. N. Mijts, and C. Schmidt-Dannert.** 2003. Biosynthesis of structurally novel carotenoids in *Escherichia coli*. Chem. Biol. **10:**453–462.

16. **Mayne, S. T.** 1996. Beta-carotene, carotenoids, and disease prevention in humans. FASEB J. **10:**690–701.

17. **Nishino, H., H. Tokuda, Y. Satomi, M. Masuda, P. Bu, M. Onozuka, S. Yamaguchi, Y. Okuda, J. Takayasu, J. Tsuruta, M. Okuda, E. Ichiishi, M. Murakoshi, T. Kato, N. Misawa, T. Narisawa, N. Takasuka, and M. Yano.** 1999. Cancer prevention by carotenoids. Pure Appl. Chem. **71:**2273–2278.

18. **Ohnuma, S., K. Narita, T. Nakazawa, C. Ishida, Y. Takeuchi, C. Ohto, and T. Nishino.** 1996. A role of the amino acid residue located on the fifth position before the first aspartate-rich motif of farnesyl diphosphate synthase in determination of the final product. J. Biol. Chem. **271:**30748–30754.

19. **Pandit, J., D. E. Danley, G. K. Schulte, S. Mazzalupo, T. A. Pauly, C. M. Hayward, E. S. Hamanaka, J. F. Thompson, and H. J. Harwood.** 2000. Crystal structure of human squalene synthase—a key enzyme in cholesterol biosynthesis. J. Biol. Chem. **275:**30610–30617.

20. **Raisig, A., and G. Sandmann.** 2001. Functional properties of diapophytoene and related desaturases of C_{30} and C_{40} carotenoid biosynthetic pathways. Biochim. Biophys. Acta Mol. Cell Biol. Lipids **1533:**164–170.

21. **Schmidt-Dannert, C., D. Umeno, and F. H. Arnold.** 2000. Molecular breeding of carotenoid biosynthetic pathways. Nat. Biotechnol. **18:**750–753.

22. **Steele, C. L., J. Crock, J. Bohlmann, and R. Croteau.** 1998. Sesquiterpene synthases from grand fir (*Abies grandis*)—comparison of constitutive and wound-induced activities, and cDNA isolation, characterization and bacterial expression of delta-selinene synthase and gamma-humulene synthase. J. Biol. Chem. **273:**2078–2089.

23. **Takaichi, S., K. Inoue, M. Akaike, M. Kobayashi, H. Ohoka, and M. T. Madigan.** 1997. The major carotenoid in all known species of heliobacteria is the C_{30} carotenoid 4,4'-diaponeurosporene, not neurosporene. Arch. Microbiol. **168:**277–281.

24. **Taylor, R. F.** 1984. Bacterial triterpenoids. Microbiol. Rev. **48:**181–198.

25. **Umeno, D., and F. H. Arnold.** 2003. A C_{35} carotenoid biosynthetic pathway. Appl. Environ. Microbiol. **69:**3573–3579.

26. **Umeno, D., K. Hiraga, and F. H. Arnold.** 2003. A method to protect the targeted amino acid residue from PCR mutagenesis. Nucleic Acids Res. **31:**e91.

27. **Umeno, D., A. V. Tobias, and F. H. Arnold.** 2002. Evolution of the C_{30} carotenoid synthase CrtM for function in a C_{40} pathway. J. Bacteriol. **184:**6690–6699.

28. **Vining, L. C.** 1992. Roles of secondary metabolites from microbes. Ciba Found. Symp. **171:**184–198.

29. **Wang, K., and S. Ohnuma.** 1999. Chain-length determination mechanism of isoprenyl diphosphate synthases and implications for molecular evolution. Trends Biochem. Sci. **24:**445–451.

30. **Wang, K. C., and S. Ohnuma.** 2000. Isoprenyl diphosphate synthases. Biochim. Biophys. Acta Mol. Cell Biol. Lipids **1529:**33–48.